Calorimetry triggering in ATLAS
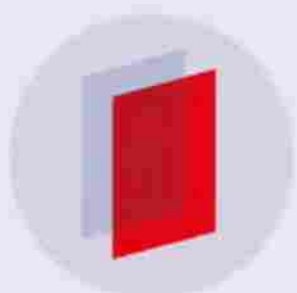
To cite this article: Igonkina O *et al* 2009 *J. Phys.: Conf. Ser.* **160** 012061

View the article online for updates and enhancements.

Calorimetry triggering in ATLAS

Igonkina O.[32], Achenbach R.[15], Adragna P.[37], Aharrouche M.[24],
Alexandre G.[11], Andrei V.[15], Anduaga X.[21], Aracena I.[41], Backlund
S.[7], Baines J.[38], Barnett B.M.[38], Bauss B.[24], Bee C.[26], Behera P.[19],
Bell P.[25], Bendel M.[24], Benslama K.[39], Berry T.[16], Bogaerts A.[7],
Bohm C.[43], Bold T.[44,9], Booth J.R.A.[5], Bosman M.[4], Boyd J.[7],
Bracinik J.[5], Brawn I.P.[38], Brelier B.[28], Brooks W.[47], Brunet S.[10],
Bucci F.[11], Casadei D.[31], Casado P.[4], Cerri A.[7], Charlton D.G.[5],
Childers J.T.[15], Collins N.J.[5], Conde Muino P.[20], Coura Torres R.[40],
Cranmer K.[31], Curtis C.J.[5], Czyczula Z.[30], Dam M.[30], Damazio D.[3],
Davis A.O.[38], De Santo A.[16], Degenhardt J.[36], Delsart P.-A.[28],
Demers S.[41], Demirkoz B.[7], Di Mattia A.[23], Diaz M.[42], Djilkibaev
R.[31], Dobson E.[34], Dova M.T.[21], Dufour M.-A.[27], Eckweiler S.[24],
Ehrenfeld W.[14,10], Eifert T.[11], Eisenhandler E.[37], Ellis N.[7],
Emeliyanov D.[38], Enoque Ferreira de Lima D.[40], Faulkner P.J.W.[5],
Ferland J.[28], Flacher H.[7], Fleckner J.E.[15], Flowerdew M.[22],
Fonseca-Martin T.[16], Fratina S.[36], Fhlisch F.[15], Gadomski S.[11],
Gallacher M.P.[5], Garitaonandia Elejabarrieta H.[32], Gee C.N.P.[38],
George S.[16], Gillman A.R.[38], Goncalo R.[16], Grabowska-Bold I.[9], Groll
M.[24], Gringer C.[24], Hadley D.R.[5], Haller J.[14,10], Hamilton A.[11],
Hanke P.[15], Hauser R.[23], Hellman S.[43], Hidvgi A.[43], Hillier S.J.[5],
Hryn'ova T.[7], Idarraga J.[28], Johansen M.[43], Johns K.[2], Kalinowski
A.[39], Khoriauli G.[39], Kirk J.[38], Klous S.[32], Kluge E.-E.[15], Koeneke
K.[10], Konoplich R.[31], Konstantinidis N.[45], Kwee R.[17], Landon M.[37],
LeCompte T.[1], Ledroit F.[13], Lei X.[2], Lendermann V.[15], Lilley J.N.[5],
Losada M.[6], Maettig S.[14,10], Mahboubi K.[15], Mahout G.[5], Maltrana
D.[42], Marino C.[18], Masik J.[25], Meier K.[15], Middleton R.P.[38], Mincer
A.[31], Moa T.[43], Monticelli F.[21], Moreno D.[6], Morris J.D.[37], Mller
F.[15], Navarro G.A.[6], Negri A.[35], Nemethy P.[31], Neusiedl A.[24],
Oltmann B.[24], Olvito D.[36], Osuna C.[4], Padilla C.[4], Panes B.[42], Parodi
F.[12], Perera V.J.O.[38], Perez E.[4], Perez Reale V.[8], Petersen B.[7],
Pinzon G.[6], Potter C.[27], Prieur D.P.F.[38], Prokishin F.[47], Qian W.[38],
Quinonez F.[42], Rajagopalan S.[3], Reinsch A.[33], Rieke S.[24], Riu I.[4],
Robertson S.[27], Rodriguez D.[6], Rogriquez Y.[6], Rhr F.[15], Saavedra
A.[46], Sankey D.P.C.[38], Santamarina C.[27], Santamarina Rios C.[27],
Scannicchio D.[35], Schiavi C.[12], Schmitt K.[15], Schultz-Coulon H.-C.[15],
Schfer U.[24], Segura E.[4], Silverstein D.[41], Silverstein S.[43], Sivoklokov
S.[29], Sjlin J.[43], Staley R.J.[5], Stamen R.[15], Stelzer J.[10], Stockton
M.C.[5], Straessner A.[11], Strom D.[33], Sushkov S.[4], Sutton M.[45],
Tamsett M.[16], Tan C.L.A.[5], Tapprogge S.[24], Thomas J.P.[5], Thompson
P.D.[5], Torrence E.[33], Tripiana M.[21], Urquijo P.[11], Urrejola P.[42],

Vachon B.[27], Vercesi V.[35], Vorwerk V.[4], Wang M.[39], Watkins P.M.[5], Watson A.[5], Weber P.[15], Weidberg T.[34], Werner P.[7], Wessels M.[15], Wheeler-Ellis S.[44], Whiteson D.[44], Wiedenmann W.[48], Wielers M.[38], Wildt M.[24], Winklmeier F.[7], Wu X.[11], Xella S.[30], Zhao L.[31], Zobernig H.[48], de Seixas J.M.[40], dos Anjos A.[48], Åsman B.[43], Özcan E.[45]

[1] Argonne National Laboratory, Argonne, Illinois
[2] University of Arizona, Tucson, Arizona
[3] Brookhaven National Laboratory (BNL), Upton, New York
[4] Institut de Fsica d'Altes Energies (IFAE), Universitat Autnoma de Barcelona, Bellaterra (Barcelona)
[5] School of Physics and Astronomy, The University of Birmingham, Birmingham
[6] Universidad Antonio Narino, Bogot, Colmbia
[7] European Laboratory for Particle Physics (CERN), Geneva
[8] Nevis Laboratory, Columbia University, Irvington, New York
[9] Faculty of Physics and Applied Computer Science, AGH University of Science and Technology, Cracow
[10] Deutsches Elektronen-Synchrotron (DESY), Hamburg and Zeuthen
[11] Section de Physique, Universit de Genve, Geneva
[12] Dipartimento di Fisica dell' Universit di Genova e I.N.F.N., Genova
[13] Laboratoire de Physique Subatomique et de Cosmologie de Grenoble (LPSC), IN2P3-CNRS-Universit Joseph Fourier, Grenoble
[14] University of Hamburg, Germany
[15] Kirchhoff Institut fr Physik, Universitt Heidelberg, Heidelberg
[16] Department of Physics, Royal Holloway and Bedford New College, Egham
[17] Institut fr Physik, Humboldt-Universitt, Berlin
[18] Indiana University, Bloomington, Indiana
[19] Iowa State University, Ames, Iowa
[20] Laboratorio de Instrumentaao e Fisica Experimental, Lisboa
[21] Universidad Nacional de La Plata, La Plata
[22] University of Liverpool, Liverpool
[23] Michigan State University, Department of Physics and Astronomy, East Lansing, Michigan
[24] Institut fr Physik, Universitt Mainz, Mainz
[25] School of Physics and Astronomy, University of Manchester, Manchester
[26] Centre de Physique des Particules de Marseille, IN2P3-CNRS, Marseille
[27] Department of Physics, McGill University, Montreal
[28] University of Montreal, Montreal
[29] Moscow State University, Moscow
[30] Niels Bohr Institute, University of Copenhagen, Copenhagen
[31] Department of Physics, New York University, New York
[32] Nikhef National Institute for Subatomic Physics, Amsterdam
[33] University of Oregon, Eugene, Oregon
[34] Department of Physics, Oxford University, Oxford
[35] Universit di Pavia, Dipartimento di Fisica Nucleare e Teorica, Pavia
[36] Department of Physics, University of Pennsylvania, Philadelphia, Pennsylvania
[37] Physics Department, Queen Mary, University of London, London
[38] STFC Rutherford Appleton Laboratory, Harwell Science and Innovation Campus, Didcot, Oxon
[39] University of Regina, Regina
[40] Universidade Federal do Rio de Janeiro, COPPE/EE/IF, Rio de Janeiro
[41] Stanford Linear Accelerator Center (SLAC), Stanford
[42] Pontificia Universidad Catlica, Santiago
[43] Fysikum, Stockholm University, Stockholm
[44] Department of Physics and Astronomy, University of California, Irvine, California
[45] Department of Physics and Astronomy, University College London, London
[46] University of Sydney, Sydney
[47] Universidad tecnica Federico Santa Maria, Valparaso
[48] Department of Physics, University of Wisconsin, Madison, Wisconsin

E-mail: `Olga.Igonkina@cern.ch`

Abstract. The ATLAS experiment is preparing for data taking at 14 TeV collision energy. A rich discovery physics program is being prepared in addition to the detailed study of Standard Model processes which will be produced in abundance. The ATLAS multi-level trigger system is designed to accept one event in $2 \cdot 10^5$ to enable the selection of rare and unusual physics events. The ATLAS calorimeter system is a precise instrument, which includes liquid Argon electro-magnetic and hadronic components as well as a scintillator-tile hadronic calorimeter. All these components are used in the various levels of the trigger system. A wide physics coverage is ensured by inclusively selecting events with candidate electrons, photons, taus, jets or those with large missing transverse energy. The commissioning of the trigger system is being performed with cosmic ray events and by replaying simulated Monte Carlo events through the trigger and data acquisition system.

1. Introduction

The ATLAS detector is a multipurpose spectrometer aiming at Standard Model precision measurements as well as discovery of physics beyond Standard Model. Operating at a center of mass energy of $\sqrt{s} \sim 14$ TeV and with a bunch crossing rate of 40 MHz, the ATLAS experiment will register unprecedentedly high number of events, most of which will contain several inelastic $p - p$ collisions. The fraction of events of interest is, however, small, as can be seen from fig. 1. The cross-section of Z and W bosons production is expected to be six orders of magnitude smaller than the rate of inelastic $p - p$ interactions, and the predictions for Higgs or Supersymmetry production are an additional three order of magnitude smaller. From the other side each recorded ATLAS event takes about 1.5MB of disk space and the storage of even small fraction of produced events requires significant capacity. To record only potentially interesting events, ATLAS is preparing a trigger system with a rejection factor of 10^5. This is 3 level system with first hardware level (L1) and with software second (L2) and third (EF) levels of *high level trigger* (HLT). The output rate is tuned to be 200Hz. Following detector design philosophy, the ATLAS trigger is a multipurpose system, oriented to select basic objects with high transverse momentum (p_T) or events with significant missing transverse energy (xE$_T$). The basic objects include electrons, photons, muons, jets and taus.

All triggers except the ones aiming at registering muons and events with B mesons, are calorimeter based. At L1, these triggers use only calorimeter, electro-magnetic and hadronic, while at higher levels the tracking information is added. For the xE$_T$ trigger also data from muon system are used at L2 and at EF. About 70% of the total bandwidth is allocated to calorimetric triggers.

2. ATLAS calorimeter and trigger system

The details of the ATLAS detector and of its calorimeters can be found elsewhere [?]. The high granularity liquid Argon (LAr) electro-magnetic (EM) sampling calorimeter covers the pseudo-rapidity range $|\eta| < 3.2$. The hadronic calorimetry (HAD) in the range $|\eta| < 1.7$ is a scintillator-tile calorimeter, which is separated into a large barrel and two smaller extended barrel cylinders, one on either side of the central barrel. In the end-caps ($|\eta| > 1.5$), LAr technology is also used for the hadronic calorimeters, matching the outer $|\eta|$ limits of end-cap electro-magnetic calorimeters. LAr forward calorimeters provide both electro-magnetic and hadronic energy measurements and extend to $|\eta| = 4.9$. The EM calorimeter is divided in four samplings around the z-axis and the hadronic part has three samplings. The total thickness of the EM calorimeter is > 22 radiation lengths in the barrel and > 24 radiation lengths in
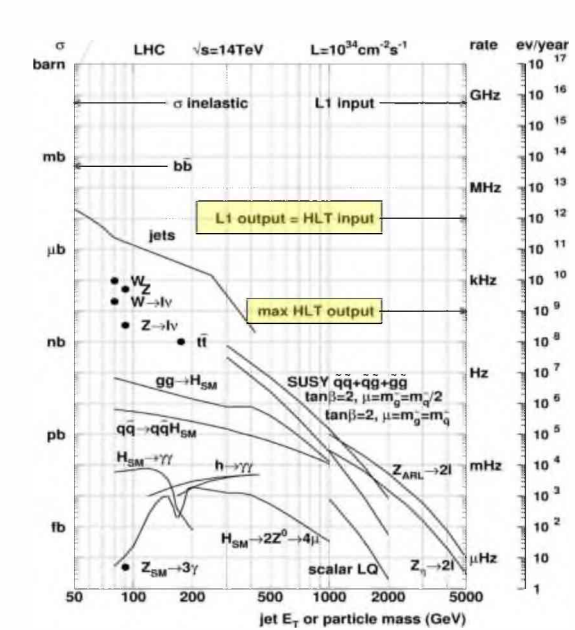
Figure 1. The expected cross-section (left axis) and corresponding event rate at $10^{34} \mathrm{cm}^{-2}$ s^{-1}instant luminosity for different processes. Also shown L1 and HLT output rates.

end-caps. The calorimeter has 9.7 interaction lengths in the barrel and 10 in the end-caps. In total there are about 175 thousand readout channels in the EM and over 15 thousand in the HAD calorimeters.

The calorimeter based trigger system covers the complete acceptance provided by the detector. The electron, photon and tau trigger cover a pseudo-rapidity region $|\eta| < 2.5$, while jet and xE_T triggers use all barrel, end-cap and forward regions.

2.1. ATLAS L1 trigger

The first level trigger is a hardware based system that reduces the rate to 75 MHz within a fixed latency of 2.5 μm. The L1 calorimeter trigger has a dedicated readout, where the energy deposition is summed in about 7000 trigger towers of $\eta \times \phi = 0.1 \times 0.1$ which are connected to FPGAs. The trigger towers are larger in the forward region. The electro-magnetic and hadronic parts of calorimeter are analyzed separately. All local maxima are considered as a trigger. The L1 trigger for electrons, photons (EM) and taus is based on 4×4 towers, while the jet trigger uses blocks of 2×2 towers and consider either 2×2, 3×3 or 4×4 blocks. L1 electron and photon triggers require a large energy deposition in the two central EM towers and limit energy deposition in the EM and HAD isolation rings as well as in HAD central 2×2 area. L1 tau trigger requires significant energy deposition in central EM and HAD areas and limits energy in EM isolation ring. L1 jet trigger cuts only on the total energy deposition of the candidate. All variables are calculated in a transverse plane. The energy summation algorithm produces also sums of E_T, E_x and E_y energy deposits over all trigger towers, which are used to construct the total E_T and missing E_T L1 triggers. Two calibrations are used at L1 - one, particle based, is applied to electron and photon candidates, while jet-based calibration is applied for all other types. The jet based calibration re-weights EM and HAD parts with an average ratio of charged and neutral pions in jets to estimate the original transverse energy of the jet.

The trigger configuration allows to set up to 16 electron/photon, 8 tau, 8 jet and 8 xE_T thresholds. The L1 trigger menu allows 256 combinations of these thresholds (*items*). In addition to physics items there are items for detector monitoring, calibration and to collect control samples. Not all of selected events, e.g. for calibration, can be recorded, therefore *prescale factors* are applied. The L1 configuration allows to use different prescale factors for the

items.

2.2. ATLAS L2 trigger

The L2 is a software trigger. The full granularity data from any sub-detectors are available within *regions of interest* (*RoI*). Usage of RoI allows to reduce the data volume at L2 nodes by about 50 times. Only fast rejection algorithms run at L2. Among them are a simple clusterization of calorimeter information and a track reconstruction algorithm. The properties of the cluster and their correlation with the number of tracks found are tested against various hypotheses. The L2 rejection of about 40 is achieved within an average event processing time of 40 ms. About one third of the time is spent on data preparation (retrieving from the pile-up buffer, decoding). Therefore it is important to avoid repetition of this operation, in case the same region of interest is requested by different trigger items. This is achieved with a *cashing* procedure, where unpacked data are stored in memory and are reused if a second call is issued. Also the results of clusterization and track reconstruction are cashed and re-used to test different hypothesis, e.g. for electron items with different p_T thresholds.

Most of electron/photon and tau cluster shape parameters are calculated using the 2nd EM sampling, while the total transverse energy deposition of taus, jets and xE_T is calculated using all 3 samplings of EM and 4 samplings of HAD calorimeter. Tracks are reconstructed and matched to the cluster for electrons, photons and taus. The L2 jet calibration takes the weight of HAD part as a logarithmic function of energy and as a function of the pseudo-rapidity. The accuracy of jet E_T reconstruction is shown on fig. 2 for different pseudo-rapidity regions. The tau trigger uses jet calibration at all trigger levels.
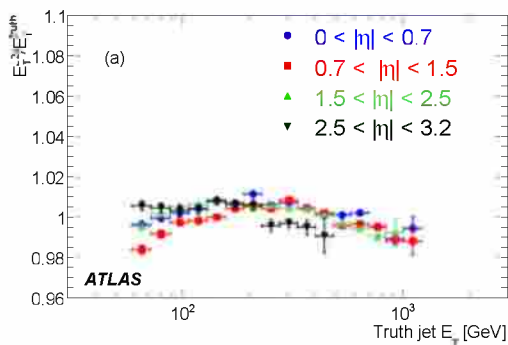

Figure 2. Jet energy scale for the L2 jets as a function of the truth jet E_T for four different bins in η..

2.3. ATLAS EF trigger

The third level trigger or *Event Filter* runs on a farm of PCs separated from L2 PCs. The complete event is built and available for analysis, however, only the data within RoIs accepted by L2 are analyzed due to time considerations. The algorithms executed are similar to the ones used for final offline reconstruction, but unlike offline reconstruction, the alignment of the various detector parts and calibration of the calorimeter are not final and are not updated during the run. The mean event processing time is about 4s and the output rate is tuned to 200Hz. The output rate is limited by the capacity of the ATLAS storage system, and although short spikes in the rate are not a problem, the average rate should not exceed design value. The data storage speed is about 300 MB/s.

More refined calibration and more advanced cuts are applied at this level. The selection cuts are optimized to provide highest possible efficiency for physics channels at the affordable rate. Different tightness cuts are introduced, such that one can use looser cuts together with prescale factor to collect control sample (e.g. for the measurement of efficiency) while tighter

cuts without any prescale are used to collect signal sample. There are L2 and EF prescale factors additional to L1 factors, in case the same L1 item is used for several HLT selections.

2.4. Trigger menu

The trigger menu is a list of items and of the corresponding prescale factors for each trigger level. It is foreseen that several menus will be deployed, one for the start-up period of LHC and the others for the different instant luminosity periods of 10^{31}, 10^{32} and 10^{33} cm^{-2} s^{-1}. The start up menu will mostly include soft L1 triggers at first, slowly migrating to more advanced HLT selection and variety of items. The 10^{31} menu is considered as a basic one for the first physics run. It will include :

- items for physics,
- items for commissioning, calibration, alignment,
- back-up triggers to be used for physics if the actual trigger rate of the chosen items will be significantly different from the expectations,
- items for the trigger efficiency measurements,
- HLT pass-through items for the debugging/monitoring of the software triggers,
- minimum bias and random triggers.

The physics goals for the first physics run at 10^{31}cm^{-2} s^{-1}are illustrated by tab. 1, where subset of unprescaled physics items are given together with expected rate at L1 and HLT and physics motivation. The complete menu for the electron trigger for 10^{31} run is shown in tab. 2. The expected rates are given for 14 TeV center-of-mass energy.

Table 1. Tentative unprescaled trigger items for 14 TeV LHC run with instant luminosity of 10^{31}cm^{-2} s^{-1}.

Signature	L1 rate (Hz)	HLT rate (Hz)	Comments
Minimum bias	Up to 10000	10	Pre-scaled trigger item
e10	5000	21	$b, c \rightarrow e, W, Z$, Drell-Yan, $t\bar{t}$
2e5	6500	6	Drell-Yan, J/ϕ, Υ, Z
γ20	370	6	Direct photons, γ -jet balance
2γ15	100	< 1	Photon pairs
mu10	360	19	$W, Z, t\bar{t}$
2mu4	70	3	B-physics, Drell-Yan, J/ϕ, Υ, Z
mu4 + $J/\phi(\mu\mu)$	1800	< 1	B-physics
j120	9	9	QCD and other high-pT jet final states
4j23	8	5	Multi-jet final states
tau20i + xE30	5000	10	$W, t\bar{t}$
tau20i + e10	130	1	$Z \rightarrow \tau\tau$
tau20i + mu6	20	3	$Z \rightarrow \tau\tau$

3. Tests of the trigger system

Various tests of the system are performed in preparation for data taking. This includes *cosmics runs* where cosmic rays are triggered with either L1 muon or L1 calorimeter and *technical runs* where L1 output is replaced with simulated data. Also, a variety of Monte Carlo tests are performed to predict change in the signal efficiencies and in the trigger rates due to imperfect detector conditions.

Table 2. Summary of triggers for the first physics run assuming a luminosity of $10^{31}\mathrm{cm}^{-2}\,\mathrm{s}^{-1}$. For each signature rates and the motivation for this trigger are given. The prescale factors are given for L1 and for HLT.

| Signature | Level-1 | | Event Filter | | | Motivation |
	Pre-scale	Rate [kHz]	Sel-ection	Pre-scale	Rate [Hz]	
e5	60	0.7	medium	1	4.8 ± 0.2	$J/\Psi \to ee$, $Y \to ee$, Drell-Yan
2e5	1	6.5	medium	1	6	$J/\psi \to ee$, $Y \to ee$, Drell-Yan
Jpsiee	1	6.5	medium	1	1	$J/\psi \to ee$, $Y \to ee$
e10	1	5.0	medium	1	21	$e^{\pm}$ from b,c decays, E/p studies
e10_xe30	1	0.2	medium	1	0.3 ± 0.3	access low p_T-range for $W \to e\nu$
2e10	1	0.5	loose	1	0.4 ± 0.2	$Z \to e^+e^-$
Zee	1	0.5	loose	1	< 0.1	$Z \to e^+e^-$
2e12i_L33	1	0.5	tight	1	< 0.1	trigger for $10^{33}\mathrm{cm}^{-2}\,\mathrm{s}^{-1}$
e15_xe20	1	0.2	loose	1	1.0 ± 0.4	access low p_T-range for $W \to e\nu$
e20_passL2	1	0.3	loose	200	< 0.1	check L2/EF performance
e20_passEF	1	0.3		125	0.1	check L2EF performance
em20_passEF	1	0.3		750	0.5 ± 0.1	check HLT performance
em20i_passEF	1	0.1		300	0.5 ± 0.1	check L1 isolation
e22i_L33	1	0.1	tight	1	1.2 ± 0.1	trigger for $10^{33}\mathrm{cm}^{-2}\,\mathrm{s}^{-1}$
em105_passHLT	1	1		1	1.0 ± 0.1	New physics, check for possible

3.1. Cosmics run

Cosmic rays interact with media of the ATLAS detector and leave hits in muon system as well as non-negligible energy deposits in the calorimeter. Although the cosmic ray traverses detector vertically and rarely crosses the interaction point, still the data are very useful to test the calorimeter readout and the L1 calorimeter response. The signals up to tens of GeV are registered in the calorimeter. The first objective of such test is to verify time and energy of the signals seen by L1 trigger which has its own dedicated readout versus signals recorded with the main calorimeter readout. Fig. 3 shows the energy deposition in the LAr and in the hadronic calorimeters versus energy reconstructed by L1. One can also see the saturation of the L1 readout in hadronic calorimeter at about 120 GeV. Another important purpose of cosmic test is to identify hot and dead calorimeter cells which might increase the trigger rate.

The calorimetric signals from the cosmics runs are also send through the L2 and EF trigger. As many triggers require tracks from the interaction point or a significant calorimetric energy deposition, no hypothesis testing is applied during the cosmics run, and most triggers are configured in *pass-through* mode, where each L1 candidate is accepted. Such exercise allows to test the data acquisition system (DAQ) and data quality monitoring procedures.

In addition to check of the trigger and DAQ performance, such tests involve large number of experts and allow to test and to prepare procedures for the operation of the detector by the shift crew and experts.

3.2. Technical runs

During the technical runs the L1 output is replaced with the simulated data. Several goals are achieved during such runs:

- test of the data acquisition system and HLT with the realistic input rate,
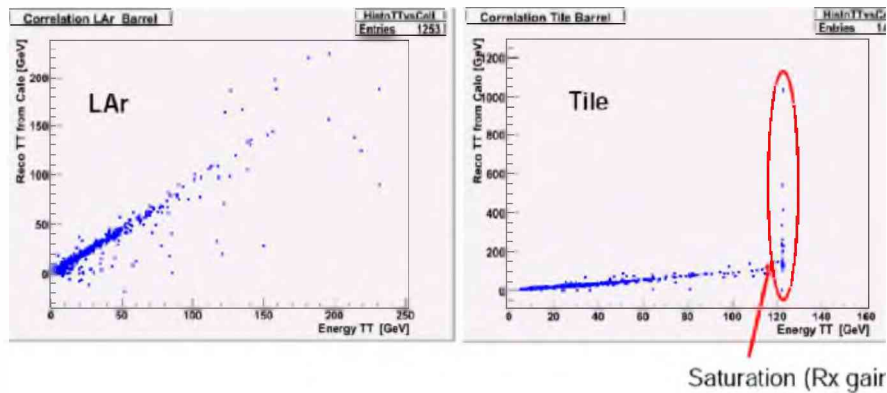
Figure 3. Energy deposition in the LAr (left) and Tile (right) barrel areas seen by detector and trigger readout during cosmics runs.

- CPU time used by the HLT algorithms as well as time required for the data preparation,
- robustness of the software triggers such as memory leaks, errors, ability to deal with incomplete data,
- stability of the performance during the long runs (usually, events are recycled many times during such long tests),
- validation of the output stream,
- ability of the data quality monitoring system to catch and report problems in timely manner,
- flexibility of tools, database access and time for initialization of the run.

The complete 10^{31} trigger menu with about 200 trigger items was successfully tested during a technical run using minimum bias events corresponding to the average detector occupancy as well as $t\bar{t}$ or events with black holes, taken as an example of the extreme occupancy.

3.3. Checks of robustness of the system
It is expected that the performance of the trigger system can be affected by a number of effects. In particular, presence of pile-up interactions or extra material in the detector can compromise the efficiency of the signal reconstruction. The misalignment of the inner-detector and the mis-calibration of calorimeter, the presence of hot and dead channels can significantly degrade the performance. Several ways are foreseen and being applied to predict behavior of the trigger and to tune algorithms such that they are less affected by a non-ideal detector response. It includes the simulation of different detector effects on Monte Carlo and the preparation of analysis software to extract efficiency from the data.

4. Estimated trigger performance
The trigger performance was studied in details in preparation for the first physics run. A large variety of physics subjects was considered, among them, searches for Higgs, Supersymmetry and a number of exotic states. The realistic description of the detector was simulated, including mis-alignment effects, imperfect response of the calorimeter readout and presence of pile-up interactions. The results could be found elsewhere [?]. In fig. 4,5,6 we give as an example, the efficiency of the main triggers of each type for the first physics run: e22i for electrons, tau16i for taus decaying hadronically, j255 for jets. Fig. 7 shows the resolution of xE_T reconstruction at different levels.
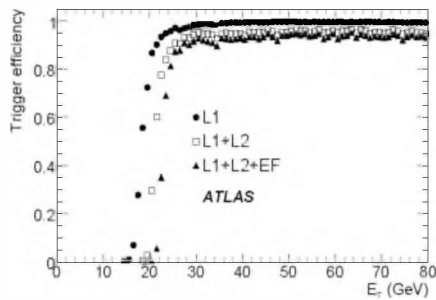
Figure 4. L1, L2 and EF efficiencies of e22i trigger item for single electrons as function of electron p_T.
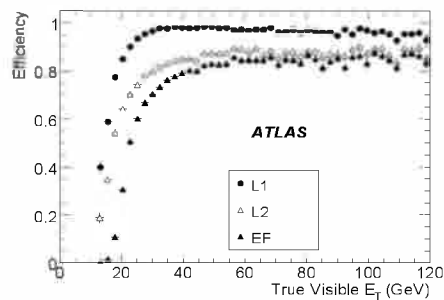

Figure 5. L1, L2 and EF efficiencies of tau16i item for the tau from W and Z bosons decaying hadronically as function of the P_T of the hadronic decay products of tau.
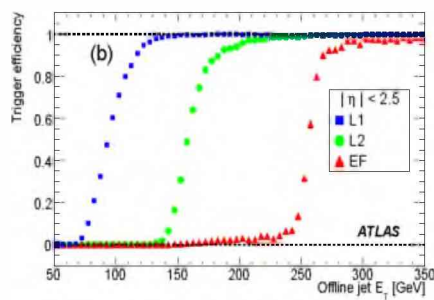

Figure 6. L1,L2 and EF efficiency of jet255 item as function of the offline jet transverse energy. The thresholds applied are 70/150/255 GeV for L1/L2/EF, respectively.
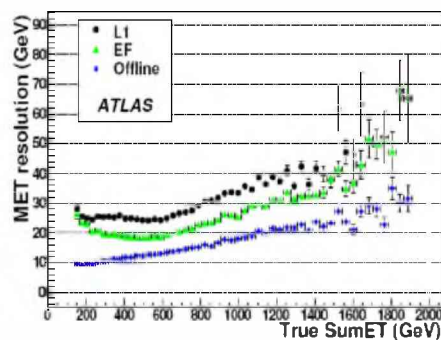

Figure 7. The resolution of xE_T as function of true sum of E_T of the event objects.

5. Conclusions

The ATLAS trigger is an advanced multipurpose system oriented to select rare events of interest out of large sample of inelastic pp events with a rejection factor of 10^5 and an output rate of 200Hz. The calorimeter is one of the main components of the system. The calorimeter based triggers take about 70% of the total output bandwidth. The ATLAS trigger consists of 3 levels: one hardware-based and two software based. All parts are installed and are being tested in preparation for the start-up of the LHC. Several types of tests are performed, among others tests of the complete system with cosmics rays and test of the HLT and DAQ with Monte Carlo events replacing L1 output.

The preparation of the trigger menu is in advanced stage with selections prepared for physics events as well as for commissioning and calibration of the detector. A set of menus are available for different luminosity periods 10^{31}, 10^{32} and 10^{33}cm^{-2} s^{-1}as well as for initial period of trigger commissioning.

[1] ATLAS Collaboration, 1999, ATLAS detector and physics performance. Technical Design report, CERN/LHCC 99-14/15
[2] ATLAS Collaboration, 2008, The ATLAS book, paper in preparation